Role of Carbonic Anhydrases in Epstein-Barr virus (EBV) induced B-cell lymphomagenesis

Submitted by

SAMARESH MALIK

Under the supervision of

Dr. Abhik Saha

Institute of Health Sciences
Presidency University, Kolkata

Contents

Introduction 1
Objectives 1
Methodology 1
Cell lines and cell culture 1
EBV stock preparation and infection of PBMCs 2
RNA sequencing and differential gene expression analysis 2
Real-time quantitative PCR (qPCR) 2
Western blot analyses 2
Fluorescence Microscopy 2
Carbonic anhydrase (CA) activity and intracellular pH assays 3
Cell viability assay 3
Colony formation assay using soft-agar 3
Transfection in epithelial and B-cells 3
Lentivirus mediated knockdown of CA9 in B-cells 3
Luciferase-based promoter assay 3
ChIP-qPCR analyses 4
Statistical analysis 4
Results 5
Objective-1: Differential gene expression analyses of carbonic anhydrases (CAs) and associated signaling molecules in response to EBV infection in B-lymphocytes. 5
Objective-2: Genetic and pharmacological ablation of identified CA isoforms to establish their role in EBV induced B-cell lymphomagenesis. 8
Objective-3: Defining underlying mechanism of transcriptional and epigenetic regulation of identified CA isoforms during EBV induced B-cell lymphoma-genesis. 10
Discussion 14
Bibliography 15

Introduction

Epstein-Barr virus (EBV) is a ubiquitus human gammaherpesvirus that asymptomatically infects over 95% of the world's population and causally linked with many cancers of epithelial and lymphoid origin[1,2]. EBV preferentially infects B-lymphocytes, leading to various B-cell malignancies such as Burkitt's lymphoma (BL), Hodgkin lymphoma (HL) and diffuse large B-cell lymphoma (DLBCL) [3]. EBV-associated malignancies are strongly associated with impaired immune system function leading to post-transplant lymphoproliferative disorders (PTLDs) in immunocompromised individuals [1,4]. EBV's life cycle involves transmuting naïve B-lymphocytes into hyperproliferating B-cell blasts followed by establishment of the latency programmes (I, II & III) through differential expression of viral oncoproteins. EBV, like other herpesviruses, has latent and lytic phases[1,2]. Viral lytic cycle replication, which maintains viral progeny, cell-to-cell spread, and host transmission, occurs during plasma cell differentiation [5]. The EBV-encoded immediate early protein BZLF1 is the main regulator for lytic cycle induction, triggering the expression of ~30 early lytic genes [6]. Lymphoblastoid cell lines (LCLs) exhibiting latency III programme are used as a surrogate model to study EBV-induced B-cell lymphomagenesis [1,7].

Carbonic anhydrases (CAs; EC 4.2.1.1) are metalloenzymes that maintain pH homeostasis of cell by producing H^+ and HCO_3^- ions in the reversible reaction $H_2O + CO_2 = H^+ + HCO_3^-$ [8,9]. Twelve enzymatically active human CA isozymes have been identified distributed in various cellular compartments - cytosolic CA1, CA2, CA3, CA7, and CA13; mitochondrial CA5A and CA5B; secretory CA6; and membrane-associated CA4, CA9, CA12, and CA14 [8]. Studies showed that cytosolic CA isoforms (CA1 and CA2) and membrane-associated CAs (CA9, CA12, and possibly CA14) cooperate to regulate tumour microenvironment pH [8]. Particularly, the membrane-associated CA isoforms convert extracellular CO_2 into HCO_3^- and H^+ ions. HCO_3^- ions are transported back into the cytoplasm and converted into CO_2, while free protons remain outside, lowering pHe. CO_2 is then used in metabolic processes or returned to the extracellular space, maintaining pHi [8]. Given the elevated expressions in different cancer types CA9 has gained much attention owing to its significant overexpression in multiple aggressive solid tumors with poor prognosis as well as association with chemotherapeutic resistance [10–15]. However, there are no reports available for B-cell lymphoma/leukaemia. In this study, we investigated the role of CA9 in EBV associated B-cell lymphomagenesis and the molecular mechanism by which CA9 assists B-cell transformation and survival.

Objectives

1. Differential gene expression analyses of carbonic anhydrases (CAs) and associated signalling molecules in response to EBV infection in B-lymphocytes.

2. Genetic and pharmacological ablation of identified CA isoforms to establish their role in EBV induced B-cell lymphomagenesis.

3. Defining underlying mechanism of transcriptional and epigenetic regulation of identified CA isoforms during EBV induced B-cell lymphomagenesis.

Methodology

Cell lines and cell culture

Cell lines were obtained from ATCC, NCCS cell repository, India or received as gifts. HEK293 and Lenti-X 293T cells were cultured in DMEM (Gibco/Invitrogen) with 10% FBS and 1% Penicillin-Streptomycin Solution. HEK293T cells with GFP-EBV BACmid cells were cultured in complete DMEM with 1 mg/ml puromycin (Sigma-Aldrich/Merck). RPMI 1640 (Gibco/Invitrogen) with 10% FBS and 1% Penicillin-Streptomycin Solution was used to maintain LCL#1 and LCL#89, P3HR1, and Jiyoye. All cells were grown at 37^0C in a humidified 5% CO_2 atmosphere unless otherwise specified.

EBV stock preparation and infection of PBMCs

GFP-tagged EBV-BACmid-expressing HEK293T cells and EBV-positive Burkitt's lymphoma cell lines P3HR1 and Jiyoye were treated with 20 ng/ml 12-O-Tetradecanoylphorbol-13-acetate (TPA) and 3 mM Sodium butyrate for 5 days to induce EBV lytic cycle replication. The viral particle was concentrated (100 x) by ultracentrifugation at 27,000 rpm for 2 hours at 4^0C and resuspended in 0.5 ml RPMI 1640 without supplementation. This virus was used for infection or stored at -80^0C. ~10 million PBMCs were in complete RPMI 1640 (0.5 million cells/ml) were incubated with GFP-EBV stock (MOI ~ 10). 24 h post-infection, cells were spun down, resuspended in fresh medium, and grown at 37^0C. Western blot and qPCR were performed on cells collected at the time points specified. For B-cell transformation experiments, PBMCs isolated from two donors were infected with GFP-EBV for 28 days in 6-well plates and subsequent B-cells blasts were photographed using a ZOE Fluorescent Cell Imager (BIO-RAD).

RNA sequencing and differential gene expression analysis

PBMCs infected with GFP-EBV and LCLs that undergone chemical EBV lytic cycle reactivation were subjected to RNA-sequencing using an Illumina NextSeq500 platform and Thermo Fisher Scientific Inc. S5 XL System, respectively. Total RNA was extracted at specific time points; libraries were prepared and sequenced following protocol. High-quality reads were then aligned to the human reference genome (Homo sapiens.GRCh37).

Differential expression analysis between two samples was conducted using DESeq2 package in R. Genes were selected based on p-value <= 0.05 and log2 Fold Change as 2 (up-regulated) or -2 (down-regulated). Differentially expressed gene sets were segregated and subsequently uploaded on DAVID v6.8 webserver for functional clustering based on Gene Ontology (GO) enrichment analysis.

Real-time quantitative PCR (qPCR)

The qPCR protocol involved extracting total RNA from approximately 10 million cells using the PureZOL™ RNA Isolation reagent, following the protocol. cDNA synthesis was carried out using the iScript cDNA synthesis kit (Bio-Rad). iTaq Supermix (Bio-Rad) was used for qPCR analysis in the CFX Connect™ real-time PCR detection system. Unless specified otherwise, each reaction was performed in triplicate, and the relative expression levels were determined using the $2^{-\Delta\Delta CT}$ method, normalized to a housekeeping gene control.

Western blot analyses

For Western blot analysis, ~10 x 10^6 cells per experiment were harvested, washed with ice-cold 1 × PBS (Gibco/Invitrogen), and lysed in 0.5 ml RIPA buffer (Thermo Fisher Scientific Inc.) with 1 x protease inhibitor cocktail (Cell Signaling Technology Inc.). The protein samples were quantified using the Bradford reagent (BIO-RAD). Following boiling in 4 x Laemmli buffer (BIO-RAD), samples were resolved by SDS-PAGE and transferred to a 0.45 μm nitrocellulose membrane. After probing specific primary antibodies followed by incubation with DyLight secondary antibodies, the membranes were analyzed using an Odyssey CLx Imaging System (LiCor Inc.).

Fluorescence Microscopy

Following each experimental procedure, cells were collected via centrifugation and subjected to two rounds of washing with 1x PBS. The cells were fixed and permeabilized using 4% paraformaldehyde (Sigma-Aldrich/Merck) and 0.1% Triton X-100. After blocking with 5% BSA (BIO-RAD) in 1 X PBS at room temperature for 1 h, cells were treated with appropriate primary antibodies for 2 h and species-specific Alexa Fluor secondary antibodies (Thermo Fisher Scientific Inc.) for 1 h. Nuclei were counterstained with 4', 6'-diamidino-2-phenylindole (DAPI; BIO-RAD) at room temperature for 30 minutes. Cells were washed three times with 1 x PBS and mounted using antifade medium (Sigma-Aldrich/Merck). The images were acquired with a Zeiss AXIO Observer.Z1 inverted fluorescence microscope and analyzed in ZEN software (Zeiss).

Carbonic anhydrase (CA) activity and intracellular pH assays

Carbonic anhydrase (CA) activity assay was performed using 5 million cells were used for each set according to the manufacturer protocol of assay kit (Abcam, USA). 5µl of CA substrate was added to each well in a 96 well plate and absorbance recorded at 405nm for 1 hour in kinetic method using BioTek Synergy microplate reader. Max-V was plotted as relative CA activity.

Intracellular pH assay was done according to kit protocol (Abcam, USA). 125,000 to 250,000 from each experiment was collected by centrifugation and dissolved in 100µl of fresh media and plated in 96 well plate. 100µl of BCFL, AM dye-loading solution was added to each well of 96 well plate and incubated 30 minutes at 37^0C followed by another 30 minutes of incubation in RT. Fluorescence was measured in a microplate reader (BioTek, USA) at Ex/Em 490/535 nm (cut off at 515 nm).

Cell viability assay

~0.5 × 105 cells plated into each well of the six-well plates (Corning Inc.) were treated with carbonic anhydrase inhibitors – SLC-0111/U-104, S4 and acetazolamide with increasing concentrations (0 – 1000 µM) for the indicated time points at 37^0C in a humidified CO_2 chamber (Thermo Fisher Scientific Inc.) or in a hypoxic environment in the presence of 1% O_2 in humidified CO_2 chamber (New Brunswick Scientific/Eppendorf) or in the presence of 300 mM $CoCl_2$ (HiMedia). Viable cells from each well were measured by Trypan blue (Gibco/Invitrogen, Inc.) exclusion method using an automated cell counter (BIO-RAD) or haemocytometer. Experiments were performed in triplicate and were independently repeated at least two times unless otherwise stated.

Colony formation assay using soft-agar

0.75% agar (Sigma-Aldrich/Merck) in 1 ml complete RPMI 1640 medium was poured into each well of 6-well plates (Corning Inc.) and set aside to solidify. Next, ~1×10^5 LCLs either left untreated (DMSO control) or treated with increasing concentrations of carbonic anhydrase inhibitors (10, 100 and 1000 µM) for 24 h, were harvested, mixed with 1 ml complete RPMI 1640 medium supplemented with 0.36% agar and poured on the top of the solidified 0.75% hard agar layer in each well. Two weeks later, colonies were stained with 0.1% crystal violet (Sigma-Aldrich/Merck) for 30 minutes and photographed (bright-field) using a ZOE Fluorescent Cell Imager (BIO-RAD). The relative colony number was measured using ImageJ2 software.

Transfection in epithelial and B-cells

Electroporation was performed in ~10 x 10^6 HEK293 ~20 x 10^6 P3HR1 cells using a Gene Pulser II electroporator (BIO-RAD) at 210 V and 975 µF for western blot, qPCR and CA activity analyses. For luciferase-based promoter assays, transfection was done by using Lipofectamine 3000 (Thermo Fisher Scientific Inc.) or JetPrime (Polyplus Transfection Inc.) according to manufacturer's protocol.

Lentivirus mediated knockdown of CA9 in B-cells

Lenti-X 293T cells were transfected with pGIPZ-sh-Cont or two different pGIPZ-sh-CA9 clones in the presence of lentivirus packaging vectors - pMDG and psPAX2 using $CaPO_4$ method as previously described [16]. 12 h post-transfection the media was removed and fresh media was added with 3 mM Sodium butyrate (Sigma-Aldrich, USA) to induce lentivirus replication. 48 h post-incubation lentivirus containing media was collected, mixed with ~5 x 10^5 Jiyoye cells in the presence of 8 µg/ml polybrene (Sigma-Aldrich/Merck) and spun at 800 g for 2 h. Transduced cells were selected with 1 µg/ml Puromycin (Sigma-Aldrich, USA) in complete RPMI for 7-days.

Luciferase-based promoter assay

Promoter assays were performed using Dual-Glo Luciferase Assay Systems kit (Promega) according to manufacturer's protocol. Briefly, ~5 x 10^5 HEK293 cells grown in 12-well plates (Corning Inc.) were transiently transfected with pGL3-CA9p promoter plasmids (wild-type or mutant) in the presence of

vector control or flag-tagged BZLF1 (wild-type) or ΔTAD-BZLF1 expressing plasmids. 36 h post-transfection, cells were lysed in 1X passive lysis reagent (PLB). 20 µl of the cell lysate was mixed with 100 µl of Luciferase Assay Reagent (LAR), and luminescence was measured in Synergy H1 microplate reader (BioTek).

ChIP-qPCR analyses

Chromatin immunoprecipitation using specific antibodies was done as previously described [17]. Briefly, 20 million cells used for cross-linking and lysis followed by sonication using an ultra-sonication processor (Diagenode, USA) for 20 cycles of 30 seconds each. The resulting soluble chromatin was diluted and incubated with a specific primary antibody (5 µg, Abcam), and then the immunocomplexes were precipitated using protein A/G beads. After extensive washing, the protein-DNA complexes were eluted from the protein A/G beads followed by reverse cross-linking through protease K treatment (40 U/ml), the DNA was purified using the QIAquick PCR purification kit (QIAGEN). Finally, the ChIP assay DNA was quantified using qPCR and normalized as a percentage of the input DNA.

Statistical analysis

All the data represented are as the mean values with standard deviation (SD). Statistical significance of differences in the mean values was analyzed using One-Way Anova (Tukey's multiple comparison test) followed by post-Dunnett test or two tailed student's t-test depending on the number of groups. The data was analyzed using Microsoft Excel and GraphPad Prism software. P-value below 0.05 was considered as significant (*$P < 0.05$; **$P < 0.01$; ***$P < 0.001$; ns, not significant).

Results

Objective-1: Differential gene expression analyses of carbonic anhydrases (CAs) and associated signaling molecules in response to EBV infection in B-lymphocytes.

Early EBV infection in naïve B-lymphocytes upregulates CA9 expression: It has been suggested that EBV infection of metabolically dormant B-lymphocytes results in a transient period of hyperproliferation during early stage of infection, resembling a germinal centre reaction [18]. During this stage, EBV-encoded oncoprotein EBNA2 through transcriptional activation of both cell and viral genes radically reprograms B-cell architecture, which in turn transforms into B-cell blasts [6,7,19]. To determine EBV induced global transcriptional alterations during this period, RNA-Seq was conducted of peripheral blood mononuclear cells (PBMCs) from a single donor infected with GFP-tagged EBV (MOI: 10) generated from a stably infected BACmid HEK293T cell line for 2-4 days (Fig. 1A-B). Gene ontology analyses demonstrated that, as expected, EBV infection provoked several known pathways, including cell division, DNA replication, cell proliferation, and glycolytic process, while repressing inflammatory and immune response signaling cascades (Fig. 1C). Among the upregulated pathways, we further investigated the expression patterns of 'cellular response to hypoxia' target genes during EBV-induced B-cell transformation (Figs. 1C and 2A-B). Previous studies suggest that EBV infection, in contrast to mitogen-induced B-cell activation, leads to the stabilization of hypoxia-induced factor 1 alpha (Hif1α), required for aerobic glycolysis [20]. Although Hif1α transcripts were present at a higher level, our RNA-Seq data indicated Hif2α (or EPAS1) was instead significantly transcriptionally activated in EBV-induced B-cell blasts as compared to the resting B-lymphocytes (Fig. 2A).

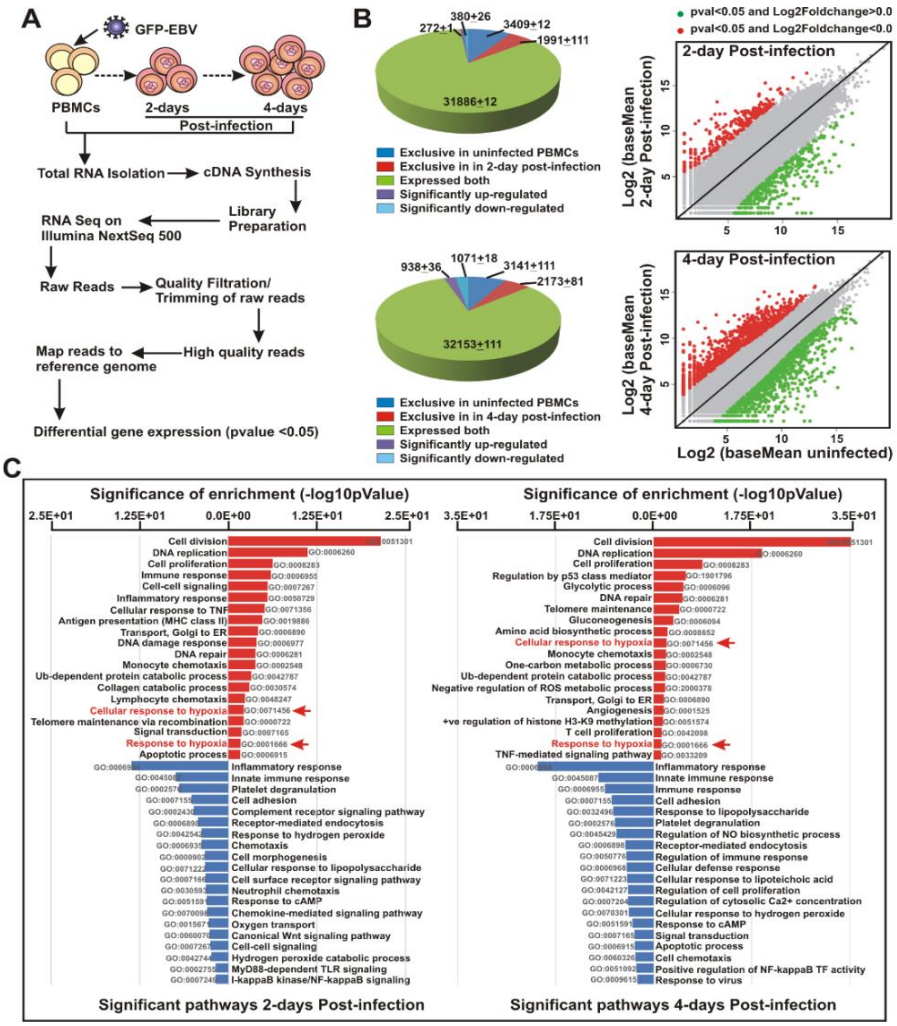

Figure 1. Whole transcriptome analysis of EBV infected resting B-cells during initial phase of infection: (A) Schematic representation (B) Pie chart and scattered plot analyses of differentially expressed genes (C) Gene Ontology (GO) analysis.

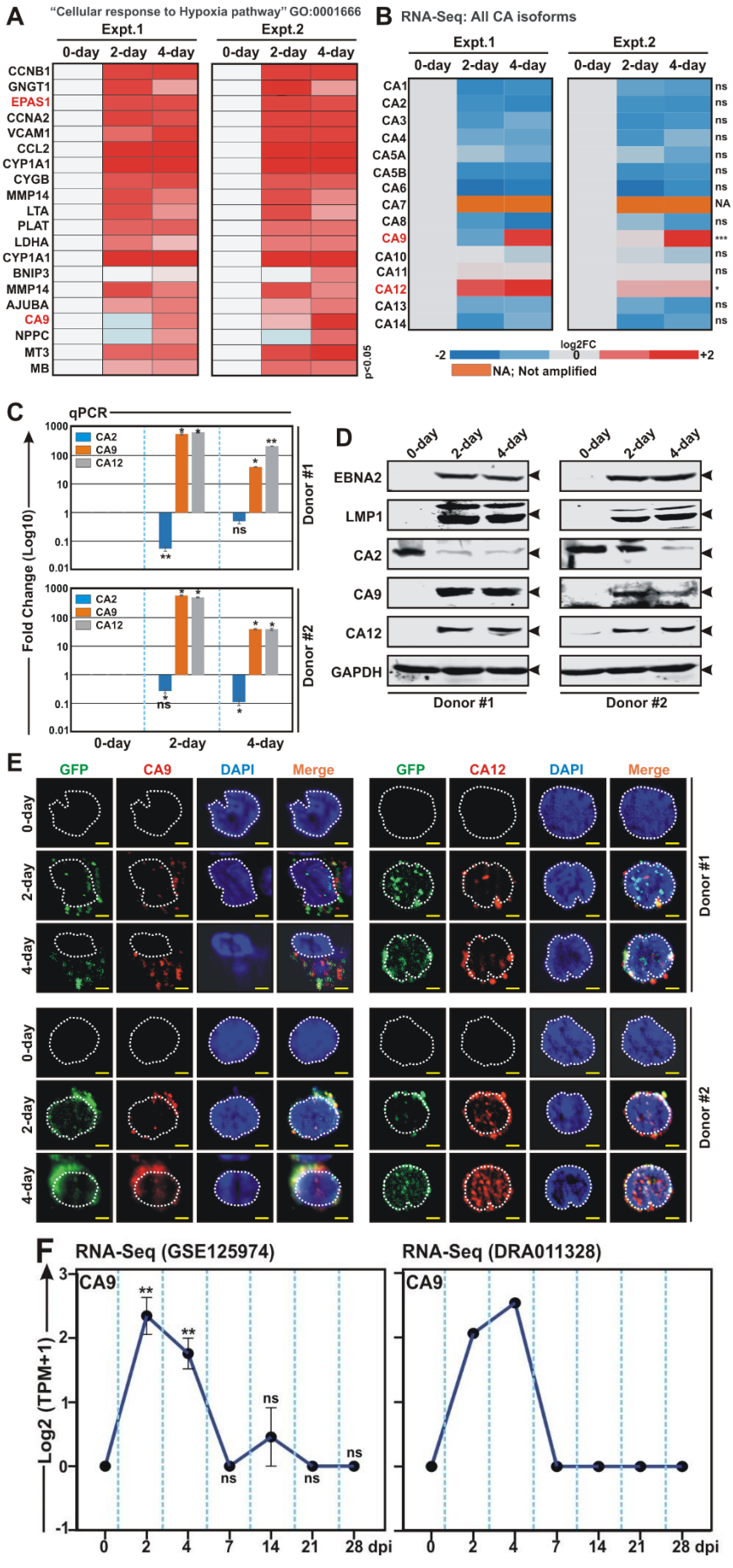

Figure 2. EBV infection of naïve B-lymphocytes specifically enhances expressions of two membrane associated carbonic anhydrase isoforms - CA9 and CA12: (A) Heat map analysis of differentially expressed genes under "Cellular response to Hypoxia pathway". (B) Heat map analysis of all CA isoforms in RNA-Seq analyses. (C-E) PBMCs from two individual donors were infected with GFP-EBV for the indicated time points and subjected to (C) quantitative real-time PCR (qPCR), (D) western blot and (E) immunofluorescence analyses. (F) Reanalysis of RNA-Seq data of B-cells infected with EBV for the indicated time points showing temporal expression prolife of CA9 transcript.

CA9, a membrane associated CA isoform, is known to be induced by hypoxia is also upregulated post EBV infection. It is known to be involved in adaptation to acidosis and implicated in cancer progression via its catalytic and/or non-catalytic functions [8,15,21]. Out of 15 CA isoforms, CA9 and to a lesser extent CA12 were significantly elevated upon EBV infection in primary B-lymphocytes (Fig. 2B) which is further supported by reanalysis of two RNA-Seq data sets (GSE125974 and DRA011328) during EBV infection of primary B-lymphocytes (Figs. 2F) which revealed only CA9 is significantly upregulated post infection. The data was further validated using two different donors in a similar experimental set up (Fig. 2C-E). Quantitative real time PCR, western blotting and immune-fluorescence studies demonstrated expressions of both CA9 and CA12 were significantly elevated in response to EBV infection in naïve B-lymphocytes (Fig. 2C-E).

EBV transformed B-lymphocytes express elevated levels of two membrane associated CA isoforms – CA9 and CA12: EBV induced transcriptional activation of CA9 and CA12 expressions during early stage of infection of naïve B-lymphocytes prompted us to further profile CA expressions in transformed B-lymphocytes. qPCR analyses of two LCLs – LCL#1 and LCL#89 demonstrated significant upregulation of only CA9 and CA12 transcripts when compared to resting B-lymphocytes (Fig. 3A-B). The transcriptional activation of CA9, CA12 and EPAS1 in LCLs was further validated by western blot analyses (Figs. 3C). Next, the transcripts profile of every member of CA and Hif family in LCLs were corroborated using the RNA-Seq data of 'Genotype-Tissue Expression (GTEx) project' (Fig. 3D). The results demonstrated that while CA2 and CA12 were downregulated, CA9 expression was significantly upregulated in EBV transformed LCLs as compared to whole blood samples (Fig. 3D). These data from primary infection and transformed B-lymphocytes models indicated CA9 might be the only prominent membrane associated CA isoform expressed in B-lymphocytes in response to EBV infection.

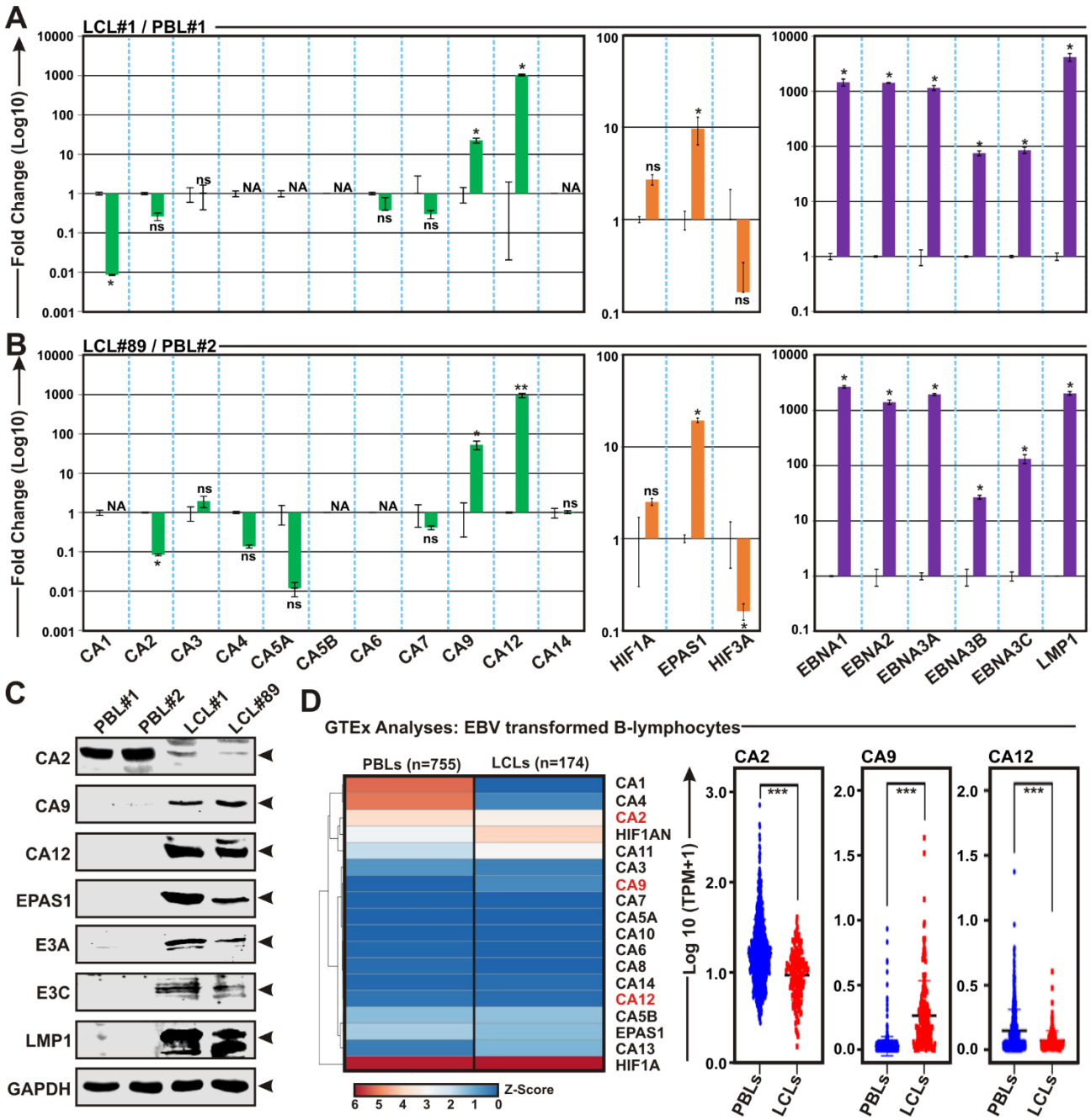

Figure 3. Elevated levels of CA9 and CA12 expressions are detected in EBV transformed B-lymphocytes: (A-B) qPCR analysis comparing relative expression of PBMCs and LCLs (C) Western blot analyses of PBMCs and LCLs (D) Heat map of whole blood cells and LCLs using (GTEx) project (https://gtexportal.org/home/).

Objective-2: Genetic and pharmacological ablation of identified CA isoforms to establish their role in EBV induced B-cell lymphomagenesis.

Carbonic anhydrase activity is required for EBV induced B-cell transformation and transformed B-cells outgrowth: Over the past two decades, CA inhibitors (CAi) against two membrane-associated CA isoforms—CA9 and CA12—have been developed as anticancer drugs due to their crucial roles in pH balance and tumor association [22,23]. Given the elevated expression pattern of CA9 and to a lesser extent CA12 in response to EBV infection, cell viability of LCLs was checked in the absence and presence of two CA9/CA12 specific inhibitors – SLC-0111/U-104 [24] and compound S4 [25] (Figs. 4). Inhibition of CA activity with increasing concentrations of both inhibitors in both the LCLs resulted in lowering of the intracellular pH, decreasing cell viability as well as colony formation ability (Figs. 4A-B). Based on

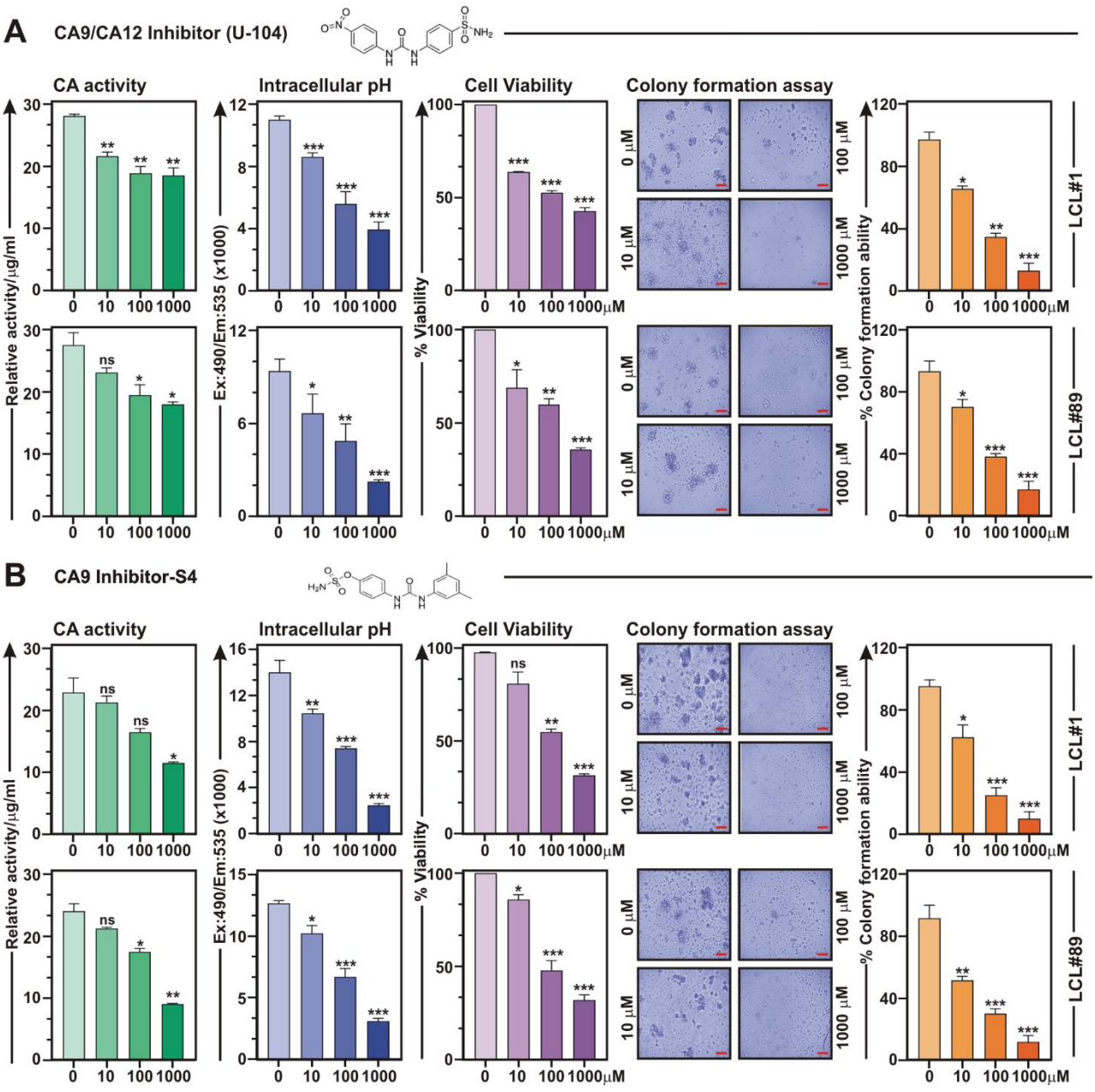

Figure 4. Carbonic anhydrase inhibitors induce cell death in EBV transformed B-lymphocytes: (A-B) LCLs were either left untreated (DMSO control) or treated with increasing concentrations (10 - 1000 µM) of CA9/CA12 specific inhibitors - (A) SLC-0111/U-104 or (B) S4 for 24 h and measured carbonic anhydrase activity, intracellular pH, cell viability and colony formation ability.

IC50 for cell viability (Figs. 4A-B) as well as inhibitor constant (Ki), compound S4 was utilized for most of the following studies.

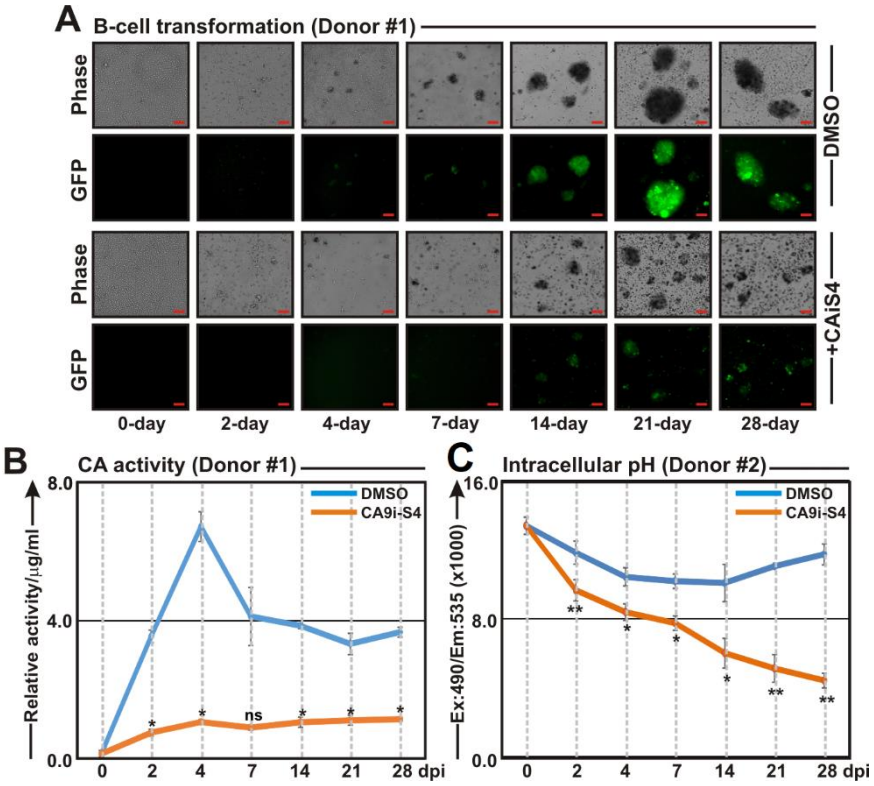

Figure 5. Carbonic anhydrase inhibitor retards EBV induced B-cell transformation: PBMCs infected with GFP-EBV in the absence or presence of 0.1 mM CAi-S4 for 28 days. (A) At the indicated time points post-infected cells were photographed using a Fluorescent Cell Imager. Scale bars, 100 µm. (C) carbonic anhydrase activity assay, (D) intracellular pH detection assay.

Next, freshly isolated PBMCs were infected with GFP-EBV (MOI: 10) in the absence and presence of CAi-S4 for 28 days to determine whether CA inhibition would hinder EBV-induced B-cell transformation. Fluorescence microscopy showed that compound S4 strongly inhibited viral B-cell transformation at each time point (0, 2, 4, 7, 14, 21 and 28 DPI) (Fig. 5A) along with significantly decreasing CA activity and intracellular pH during EBV-induced B-cell transformation (Figs. 5B and 5C). These results suggest that early EBV infection alters CA9 expression and activity to facilitate the physiological shift from quiescence to rapid lymphoblastic progression.

To determine whether elevated CA9 expression is required for B-cell growth, CA9 expression was knocked-down using two specific sh-RNAs. The efficiency of CA9 knockdown by sh-RNA in stably transduced Jiyoye cells was confirmed by western blot and qPCR analyses (Figs. 6A-B). The knockdown of CA9 resulted in significant reduction of both CA activity and intracellular pH (Figs. 6C-D). To understand whether CA9 knockdown had any effect on cell growth we conducted cell proliferation assay which revealed significant retardation of cell proliferation in Jiyoye cells (Figs. 6E). Overall, the results indicated that CA9 activity is important for EBV induced B-cell proliferation, and survival.

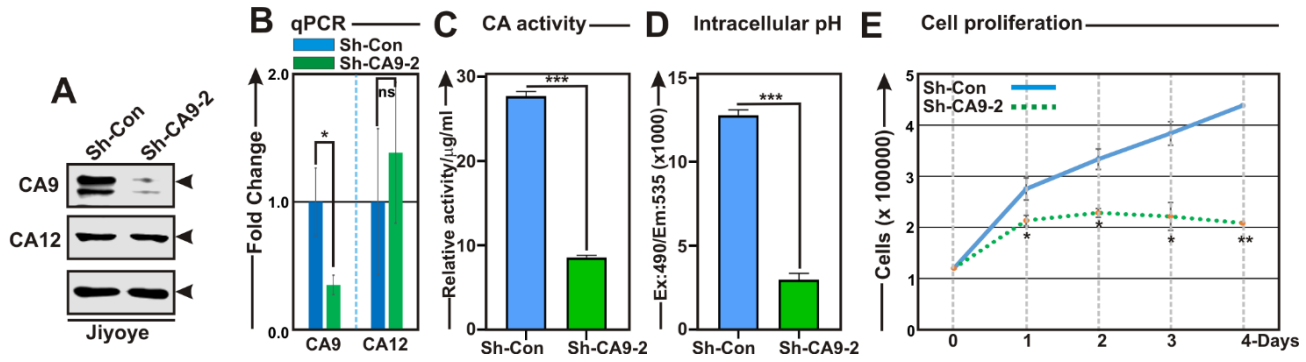

Figure 6. sh-RNA mediated knockdown of CA9: Jiyoye cells stably transduced with lentiviruses expressing either sh-control or sh-RNA) against CA9 gene were subjected to (A) western blot, (B) qPCR, (C) carbonic anhydrase activity, (D) intracellular pH and (E) cell proliferation analyses.

Objective-3: Defining underlying mechanism of transcriptional and epigenetic regulation of identified CA isoforms during EBV induced B-cell lymphoma-genesis.

EBV oncoprotein EBNA2 and B-cell specific transcription factors are recruited on to distal CA9 promoter/enhancer region: To understand the underlying molecular mechanism governing CA9 transcriptional activation, ChIP-Seq data was reanalyzed for all six EBNA proteins - EBNA1, EBNA2, EBNALP, EBNA3A, EBNA3B and EBNA3C along with several B-cell specific transcription factors. LMP1 constitutively activates NF-κB to promote LCLs growth and survival [26,27] and therefore ChIP-Seq data for NF-κB subunits were also included (Fig. 7A). Reanalysis of ChIP-Seq data revealed that among

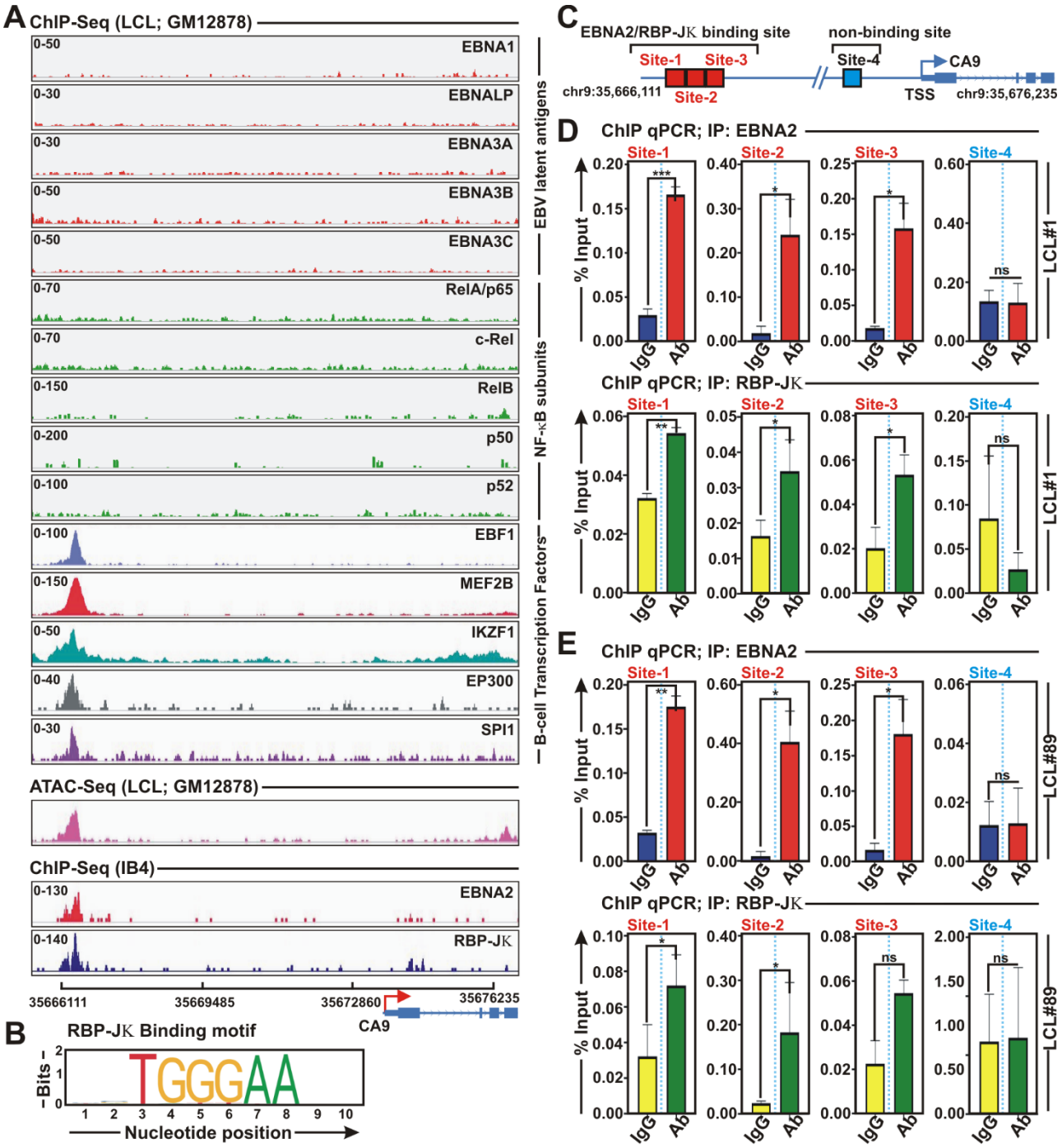

Figure 7. EBNA2 and several B-cell specific transcriptional factors colocalize onto CA9 promoter region: (A) Reanalysis of ChIP-seq data from public datasets (B) RBP-Jκ binding motif (C) genomic location for three RBP-Jκ binding and non-binding sites on the CA9 promoter region (D-E) ChIP-qPCR showing recruitment of (D) EBNA2 and (E) RBP-Jκ on CA9 promoter region.

all the viral genes only EBNA2 peak in all the ChIP-Seq data was significantly enriched onto CA9 promoter/enhancer region (Figs. 7A). EBNA2 peak also converged with several B-cell specific transcription factors including RBP-Jκ, EBF1, MEF2B, EP300 and SPI1 (Fig. 7A). Reanalysis of ATAC-Seq data in LCL GM12878 also demonstrated chromatin accessibility in the EBNA2 binding region (Fig. 7A), indicating a plausible transcriptional regulation of CA9 expression at the distal promoter/enhancer region via recruiting distinct B-cell specific transcription factors.

Among the enriched transcription factors, previous genome wide analyses demonstrated RBP-Jκ had highest co-occupancy with EBNA2 binding regions [28]. To examine whether EBNA2 and RBP-Jκ interaction is necessary for CA9 transcription, the presence of putative RBP-Jκ binding sites in the CA9 promoter/enhancer region analyzed by JASPAR. Three distinct putative RBP-Jκ binding motifs were identified in the distal EBNA2 binding region (Fig. 7B). To further confirm co-occupancy of EBNA2 and RBP-Jκ on the CA9 promoter region, three primer sets were designed for the distal binding and one primer set for the proximal non-binding regions of CA9 to perform ChIP-qPCR in two LCLs- LCL#1 and LCL#89 (Fig. 7C). Overall, the results demonstrated that both EBNA2 and RBP-Jκ were significantly enriched at all three distal binding sites, while no binding was observed in the proximal non-binding region of CA9 promoter in both LCLs (Figs. 7D and 7E, respectively).

EBNA2 mediated CA9 expression is essential for B-cell survival: EBNA2 recruitment onto CA9 promoter/enhancer region prompted to investigate if loss of EBNA2 gene expression abrogates CA9 expression and activity during primary B-lymphocyte EBV infection. For this, viruses were isolated from two EBV-positive Burkitt's lymphoma lines, P3HR1 and Jiyoye, and infected PBMCs for 2 and 4 days (Fig. 8A). While P3HR1 contains type 2 EBV strain with naturally occurring EBNA2 deletion, Jiyoye harbours wild-type type 2 EBV strain [29,30]. qPCR analyses of PBMCs infected with either P3HR1 (ΔEBNA2) or Jiyoye (wild-type) virus demonstrated that EBNA2 expression was directly correlated with CA9 but not with CA12 expressions (Fig. 8B). Elevated CA9 expression was further correlated with higher CA activity and unaltered intracellular pH in wild-type virus infected PBMCs when compared with ΔEBNA2 virus infected PBMCs (Fig. 8C-D), indicating that EBNA2 mediated CA9 expression plays an important role during early stage of EBV induced B-cell activation. Western blot analyses of P3HR1 and Jiyoye cells evidently demonstrated that EBNA2 expression was directly

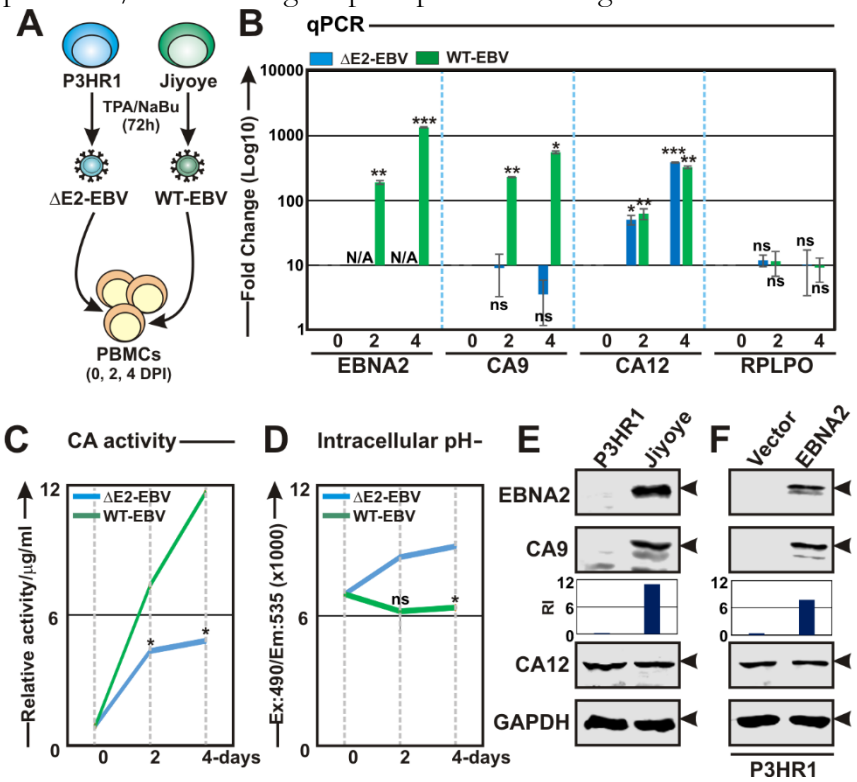

Figure 8. EBNA2 mediated CA9 transcriptional activation is essential for B-cell survival: (A-D) PBMCs infected with EBNA2 deleted and wild-type EBV generated from P3HR1 and Jiyoye cells, respectively, were subjected to (B) qPCR, (C) carbonic anhydrase activity and (D) intracellular pH analyses. (E) Comparative analyses of P3HR1 and Jiyoye cells by western blot, (F) P3HR1 cells transiently transfected with EBNA2 overexpressing pSG5-EBAN2 construct.

interrelated with elevated CA9 expressions, while CA12 expressions were unaltered in these two lines (Fig. 8E).

A more direct correlation between EBNA2 and CA9 expressions was further established utilizing P3HR1 null EBNA2 cell line transiently transfected with vector control or EBNA2 expressing plasmid (Fig. 8F). The results demonstrated that EBNA2 expression stimulated CA9 expression, which was typically absent in P3HR1 cells (Fig. 8F).

EBV lytic cycle reactivation leads to CA9 downregulation: While latent EBV infection in quiescent B-lymphocytes leads to B-cell activation, which ultimately develops B-cell lymphomas [1,7], EBV reactivation into lytic replication is essential to maintain the production of progeny virus and viral transmission from one host to another [31]. Elevated CA9 expression during EBV latent infection, prompted us to further investigate CA9 expression pattern during lytic cycle reactivation. Chemically Induction EBV lytic cycle in two LCLs followed by RNA-Seq analyses of 0, 48 and 72 h post-treatment LCLs revealed transcriptional repression of only CA9 among all fifteen CA isoforms (Fig. 9A-C). The immediate early factor BZLF1, the master regulator of EBV lytic cycle, triggers expression of ~30 early lytic genes through transcriptional activation, important for lytic DNA replication [32,33]. qPCR and western blot analyses further confirmed CA9 repression and BZLF1 activation in response to chemically induced

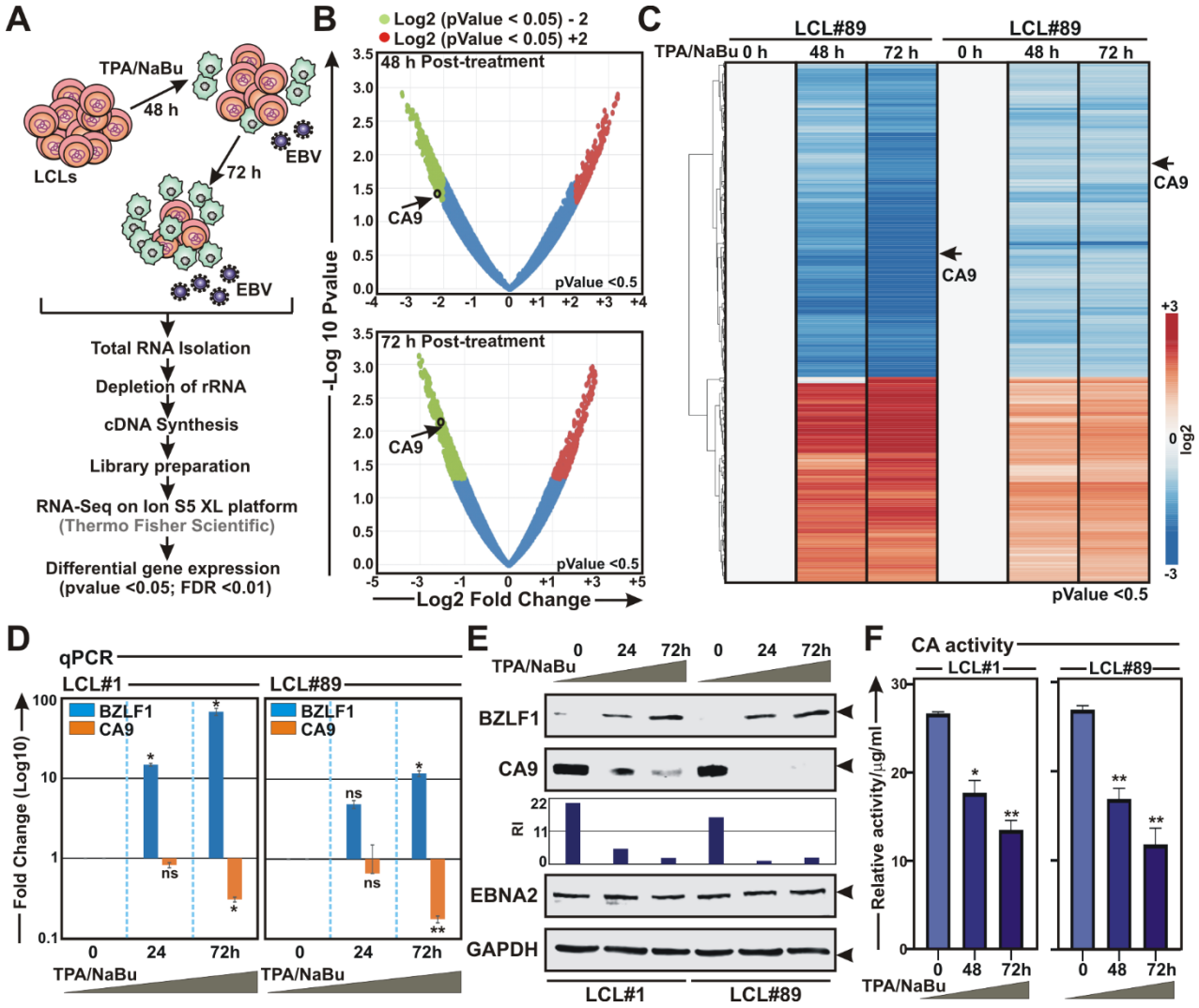

Figure 9. RNA-Seq analyses of EBV lytic cycle reactivation from LCLs reveal CA9 downregulation: (A-C) Whole transcriptome analysis of LCLs reactivated to lytic cycle replication (B-C) Volcano plot and heat map analyses of differentially expressed gene sets at 48 and 72 h post-induction. (D-F) LCLs reactivated to lytic cycle replication in a similar experimental set up were subjected to (D) western blot, (E) qPCR and (F) carbonic anhydrase activity analyses.

EBV lytic cycle replication in both LCLs. (Figs. 9D and 9E, respectively). Downregulation of CA9 expression also directly correlated with significant decrease in CA activity during viral lytic cycle reactivation in a dose dependent manner (Fig. 9F). It was hypothesized that in contrast to B-cell transformation, suppression of CA9 expression and its activity might play an essential role in supporting the viral lytic cycle reactivation.

EBV lytic cycle transactivator BZLF1 specifically downregulates CA9 expression: Next, to check whether BZLF1 induction during lytic cycle replication is directly responsible for CA9 transcriptional repression, first, HEK293 cells were transiently transfected with flag-tagged BZLF1 and results demonstrated that BZLF1 expression was inversely correlated with CA9 expression in a dose dependent fashion at both transcript and protein levels (Figs. 10A and 10B, respectively) was further corroborated with decreasing CA activity in a dose dependent manner (Fig. 10C). ChIP-Seq reanalysis (E-MTAB-7788) of Raji cells stably expressing BZLF1 [34] revealed several distinct BZLF1 ChIP-Seq signals in the CA9 promoter region (Fig. 10D). Subsequently, the ChIP-Seq peaks identified by MACS2 peak calling in the CA9 promoter were examined for AP1-like BZLF1 binding motifs [35,36], leading to the identification of several BZLF1 binding sites (Fig. 10D). ChIP-qPCR analyses using Jiyoye cells with or without EBV lytic cycle reactivation confirmed there was a significant enrichment of BZLF1 binding at both sites upon lytic cycle reactivation in Jiyoye cells (Fig. 10E).

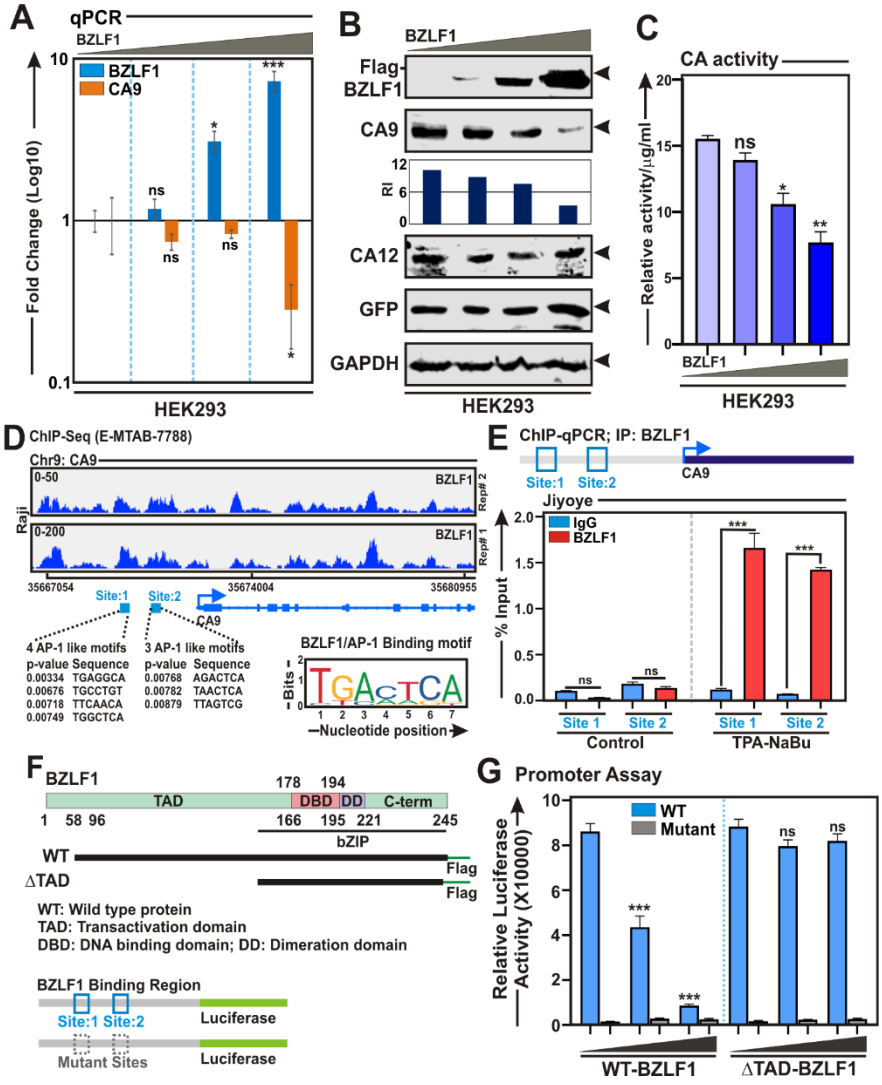

Figure 10. EBV lytic cycle master regulator BZLF1 transcriptionally represses CA9 expression: (A-C) ~10 x 106 HEK293 transfected increasing concentrations of pA3F-BZLF1 subjected to (A) qPCR, (B) western blot and (C) carbonic anhydrase activity analyses. (D) Reanalyses of ChIP-Seq data (E-MTAB-7788) showing enrichment of BZLF1 on CA9 promoter region. Schema showing BZLF1 homologue AP-1 binding motifs on the MACS identified peaks of CA9 promoter region. (E) ChIP-qPCR data showing recruitment of BZLF1 on the CA9 promoter upon EBV lytic cycle reactivation (F) Schema illustrating known structural domains of BZLF1 and CA9 promoter region (K) Luciferase reporter activity of the wild-type and mutant CA9 promoters in transiently transfected HEK293 cells.

Studies suggest that chromatin accessibility by BZLF1 strictly depends on its transactivation domain (TAD), while basic leucine-zipper (bZIP) domain alone, that is, BZLF1 lacking its TAD demonstrates similar DNA binding ability [37]. To directly validate BZLF1 mediated CA9 transcriptional repression, ΔTAD and ΔbZIP BZLF1 constructs was generated (Fig. 10F). Luciferase based promoter assay using wild type or mutant BZLF1 binding sites in the absence and

presence of either wild-type or ΔTAD BZLF1 proteins demonstrated that while wild-type BZLF1 transcriptionally repressed CA9 promoter activity in a dose dependent manner, ΔTAD BZLF1 did not show any transcriptional repression (Fig. 10G).

Overall, the results are consistent with a model (Fig. 11) in which during EBV latent infection of nascent B-lymphocytes, EBNA2 transcriptionally activates CA9 expression, while intermittent transition of latent phase to lytic replication cycle by BZLF1 transcriptionally represses CA9 expression and its activity.

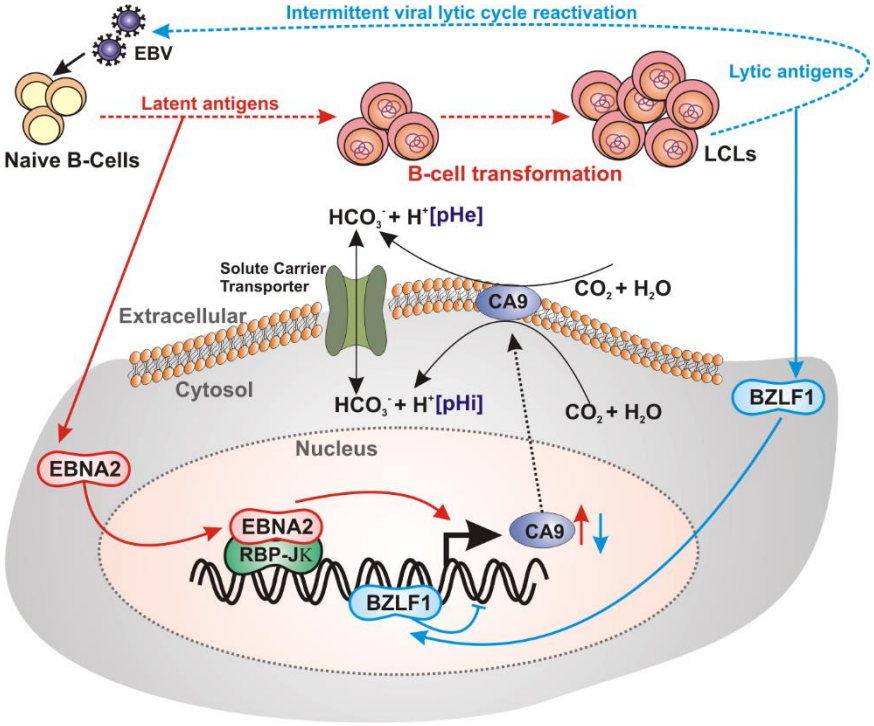

Figure 11. Schematic representation of EBV mediated dynamic CA9 expression and pH regulation during B-cell transformation and lytic cycle reactivation.

Discussion

Metabolic reprogramming and acid-base regulation are one of the major hallmarks of cancer development[38,39]. The acidic shift in the extracellular tumour microenvironment fosters cancer cell proliferation by outcompeting their adjacent host cells along with increasing metastatic potential and chemotherapeutic resistance [40,41]. CA isoforms catalyse the reaction $CO_2 + H_2O \rightleftarrows HCO_3^- + H^+$ and maintain the acid-base homeostasis [8]. Out of the twelve human CAs, two membrane associated CA isoforms – CA9 and CA12 have been largely implicated in cancer development, particularly in case of solid cancers [10–15,21,42–45]. In contrast, expression profile and the associated functions of these CA isoforms have not been extensively studied in B-cell lymphoma [46]. Being a lymphotropic virus, EBV has been shown to be associated with the development of several B-cell malignancies. Despite the strong connection with cancer cell metabolic reprogramming and acid-base balance, to date, there are no studies demonstrating a role of any CA isoforms during EBV induced B-cell transformation and subsequent B-cell lymphoma development. This study demonstrated a positive correlation of elevated CA9 expression with latent EBV infection in nascent B-lymphocytes. The results together with reanalyses of several RNA-Seq data available in the public domain further validated that CA9 was significantly associated with EBV induced B-cell transformation, particularly during early phase of viral infection event (2-4 DPI). This study also demonstrated that EBNA2 is responsible for CA9 transcriptional activation. EBNA2 typically interacts with DNA through sequence-specific transcription factor RBP-Jκ, a key mediator of Notch signalling pathway, and thereby activating cell/viral gene transcription [47,48].

Given their elevated expression in multiple cancers and prominent roles in extracellular acidification of the tumour microenvironment resulting in increasing metastatic potential and decreasing the efficacy of chemotherapy, CA9/CA12 specific inhibitors are currently emerging as potential anti-cancer drugs particularly for the treatment of solid cancers [22,23]. Through utilizing two CA9/CA12 specific inhibitors (39-41), the data indicated that this membrane associated CA isoforms, particularly CA9, are important for EBV induced B-cell transformation and LCLs outgrowth. The essential role of CA9 expression in EBV positive B-cells was also confirmed by knocking down CA9 expression through utilizing two specific Sh-RNAs.

While latent EBV infection of naïve B-lymphocytes causes B-cell activation, leading to B-cell blasts [1,2], intermittent lytic cycle reactivation is important for production of viral progeny as well as transmission from one host to another [31]. Given its importance in EBV pathogenesis, inhibition of EBV lytic replication may therefore serve as a treatment strategy for EBV-associated malignancies [32]. This study demonstrated that in contrast to EBV latent infection, lytic cycle reactivation caused a significant decrease in CA9 expression. Mechanistically, this data showed that BZLF1 transcriptionally repressed CA9 expression through direct binding onto its promoter region.

In sum, the current model portrays a differential CA9 expression during EBV pathogenesis. While during EBV latent infection elevated CA9 functions appears to be necessary for efficient B-cell transformation and survival of transformed B-lymphocytes, intermittent switch to lytic replication cycle blocks its activity. It is not yet clear, whether CA9 expression may control the EBV latent to lytic cycle transition. Future studies should focus in identifying the role of CA9 in regulating EBV latent to lytic switch and potential use of CA inhibitors for lytic induction therapy against multiple EBV associated B-cell lymphomas.

Bibliography

1. Saha, A. & Robertson, E. S. Mechanisms of B-Cell Oncogenesis Induced by Epstein-Barr Virus. *J Virol* **93**, (2019).
2. Young, L. S., Yap, L. F. & Murray, P. G. Epstein-Barr virus: more than 50 years old and still providing surprises. *Nat Rev Cancer* **16**, 789–802 (2016).
3. Shannon-Lowe, C., Rickinson, A. B. & Bell, A. I. Epstein-Barr virus-associated lymphomas. *Philos Trans R Soc Lond B Biol Sci* **372**, (2017).
4. Kang, M. S. & Kieff, E. Epstein–Barr virus latent genes. *Experimental & Molecular Medicine 2015 47:1* **47**, e131–e131 (2015).
5. Styles, C. T. *et al.* EBV epigenetically suppresses the B cell-to-plasma cell differentiation pathway while establishing long-term latency. *PLoS Biol* **15**, e2001992 (2017).
6. Guo, R. *et al.* Methionine metabolism controls the B cell EBV epigenome and viral latency. *Cell Metab* **34**, 1280-1297.e9 (2022).
7. Burton, E. M. & Gewurz, B. E. Epstein–Barr virus oncoprotein–driven B cell metabolism remodeling. *PLoS Pathog* **18**, e1010254 (2022).
8. Mboge, M. Y., Mahon, B. P., McKenna, R. & Frost, S. C. Carbonic Anhydrases: Role in pH Control and Cancer. *Metabolites* **8**, (2018).
9. Occhipinti & Boron. Role of Carbonic Anhydrases and Inhibitors in Acid–Base Physiology: Insights from Mathematical Modeling. *Int J Mol Sci* **20**, 3841 (2019).
10. Capkova, L., Koubkova, L. & Kodet, R. Expression of carbonic anhydrase IX (CAIX) in malignant mesothelioma. An immunohistochemical and immunocytochemical study. *Neoplasma* **61**, 161–169 (2014).
11. Huang, W. J. *et al.* Expression of Hypoxic Marker Carbonic Anhydrase IX Predicts Poor Prognosis in Resectable Hepatocellular Carcinoma. *PLoS One* **10**, e0119181 (2015).

12. Jomrich, G. *et al.* Stromal expression of carbonic anhydrase IX in esophageal cancer. *Clin Transl Oncol* **16**, 966–972 (2014).
13. Li, G. *et al.* CA9 as a biomarker in preoperative biopsy of small solid renal masses for diagnosis of clear cell renal cell carcinoma. *Biomarkers* **22**, 123–126 (2017).
14. Yang, J. S. *et al.* Carbonic anhydrase IX overexpression regulates the migration and progression in oral squamous cell carcinoma. *Tumour Biol* **36**, 9517–9524 (2015).
15. Yang, J. S. *et al.* Increased expression of carbonic anhydrase IX in oral submucous fibrosis and oral squamous cell carcinoma. *Clin Chem Lab Med* **52**, 1367–1377 (2014).
16. Kumar, P., Nagarajan, A. & Uchil, P. D. Calcium Phosphate-Mediated Transfection of Adherent Cells or Cells Growing in Suspension: Variations on the Basic Method. *Cold Spring Harb Protoc* **2019**, pdb.prot095455 (2019).
17. Guo, R. *et al.* DNA Methylation Enzymes and PRC1 Restrict B-cell Epstein-Barr Virus Oncoprotein Expression. *Nat Microbiol* **5**, 1051 (2020).
18. McFadden, K. *et al.* Metabolic stress is a barrier to Epstein-Barr virus-mediated B-cell immortalization. *Proc Natl Acad Sci U S A* **113**, E782–E790 (2016).
19. Wang, L. W. *et al.* Epstein-Barr-Virus-Induced One-Carbon Metabolism Drives B Cell Transformation. *Cell Metab* **30**, 539-555.e11 (2019).
20. Darekar, S. *et al.* Epstein-Barr virus immortalization of human B-cells leads to stabilization of hypoxia-induced factor 1 alpha, congruent with the Warburg effect. *PLoS One* **7**, (2012).
21. Jamali, S. *et al.* Hypoxia-induced carbonic anhydrase IX facilitates lactate flux in human breast cancer cells by non-catalytic function. *Scientific Reports 2015 5:1* **5**, 1–16 (2015).
22. Kciuk, M. *et al.* Targeting carbonic anhydrase IX and XII isoforms with small molecule inhibitors and monoclonal antibodies. *J Enzyme Inhib Med Chem* **37**, 1278–1298 (2022).
23. Mboge, M. Y., McKenna, R. & Frost, S. C. Advances in Anti-Cancer Drug Development Targeting Carbonic Anhydrase IX and XII. *Top Anticancer Res* **5**, 3 (2015).
24. McDonald, P. C. *et al.* A Phase 1 Study of SLC-0111, a Novel Inhibitor of Carbonic Anhydrase IX, in Patients With Advanced Solid Tumors. *Am J Clin Oncol* **43**, 484–490 (2020).
25. Williams, K. J. & Gieling, R. G. Preclinical Evaluation of Ureidosulfamate Carbonic Anhydrase IX/XII Inhibitors in the Treatment of Cancers. *Int J Mol Sci* **20**, (2019).
26. Lavorgna, A. & Harhaj, E. W. EBV LMP1: New and shared pathways to NF-κB activation. *Proceedings of the National Academy of Sciences* **109**, 2188–2189 (2012).
27. Zhou, H. *et al.* Epstein-Barr virus oncoprotein super-enhancers control B cell growth. *Cell Host Microbe* **17**, 205–216 (2015).
28. Zhao, B. *et al.* Epstein-Barr virus exploits intrinsic B-lymphocyte transcription programs to achieve immortal cell growth. *Proc Natl Acad Sci U S A* **108**, 14902–14907 (2011).
29. Braun, T. *et al.* Non-viral TRAC-knocked-in CD19KICAR-T and gp350KICAR-T cells tested against Burkitt lymphomas with type 1 or 2 EBV infection: In vivo cellular dynamics and potency. *Front Immunol* **14**, 1086433 (2023).
30. Cohen, J. I., Wang, F., Mannick, J. & Kieff, E. Epstein-Barr virus nuclear protein 2 is a key determinant of lymphocyte transformation. *Proc Natl Acad Sci U S A* **86**, 9558 (1989).
31. Kerr, J. R. Epstein-Barr virus (EBV) reactivation and therapeutic inhibitors. *J Clin Pathol* **72**, 651–658 (2019).
32. Li, H. *et al.* Therapies based on targeting Epstein-Barr virus lytic replication for EBV-associated malignancies. *Cancer Sci* **109**, 2101 (2018).
33. Guo, R. *et al.* MYC Controls the Epstein-Barr Virus Lytic Switch. *Mol Cell* **78**, 653-669.e8 (2020).
34. Buschle, A. *et al.* Epstein-Barr virus inactivates the transcriptome and disrupts the chromatin architecture of its host cell in the first phase of lytic reactivation. *Nucleic Acids Res* **49**, 3217–3241 (2021).
35. Baumann, M. *et al.* Activation of the Epstein-Barr Virus Transcription Factor BZLF1 by 12-O-Tetradecanoylphorbol-13-Acetate-Induced Phosphorylation. *J Virol* **72**, 8105 (1998).

36. Bernaudat, F. *et al.* Structural basis of DNA methylation-dependent site selectivity of the Epstein–Barr virus lytic switch protein ZEBRA/Zta/BZLF1. *Nucleic Acids Res* **50**, 490–511 (2022).
37. Schaeffner, M. *et al.* BZLF1 interacts with chromatin remodelers promoting escape from latent infections with EBV. *Life Sci Alliance* **2**, (2019).
38. Lagadic-Gossmann, D., Huc, L. & Lecureur, V. Alterations of intracellular pH homeostasis in apoptosis: Origins and roles. *Cell Death Differ* **11**, 953–961 (2004).
39. Matsuyama, S., Llopis, J., Deveraux, Q. L., Tsien, R. Y. & Reed, J. C. Changes in intramitochondrial and cytosolic pH: early events that modulate caspase activation during apoptosis. *Nat Cell Biol* **2**, 318–325 (2000).
40. Bogdanov, A. *et al.* Tumor acidity: From hallmark of cancer to target of treatment. *Front Oncol* **12**, (2022).
41. Kato, Y. *et al.* Acidic extracellular microenvironment and cancer. *Cancer Cell Int* **13**, 89 (2013).
42. Smith, A. D. *et al.* The Utility of Serum CA9 for Prognostication in Prostate Cancer. *Anticancer Res* **36**, 4489–4492 (2016).
43. Li, G. *et al.* Carbonic Anhydrase XII is a Clinically Significant, Molecular Tumor-Subtype Specific Therapeutic Target in Glioma with the Potential to Combat Invasion of Brain Tumor Cells. *Onco Targets Ther* **14**, 1707 (2021).
44. Ning, W. R. *et al.* Carbonic anhydrase XII mediates the survival and prometastatic functions of macrophages in human hepatocellular carcinoma. *J Clin Invest* **132**, (2022).
45. De Martino, M. *et al.* Carbonic anhydrase IX as a diagnostic urinary marker for urothelial bladder cancer. *Eur Urol* **68**, 552–554 (2015).
46. Chen, L. Q. *et al.* Assessment of carbonic anhydrase IX expression and extracellular pH in B-cell lymphoma cell line models. *Leuk Lymphoma* **56**, 1432–1439 (2015).
47. Lake, R. J., Tsai, P.-F., Choi, I., Won, K.-J. & Fan, H.-Y. RBPJ, the Major Transcriptional Effector of Notch Signaling, Remains Associated with Chromatin throughout Mitosis, Suggesting a Role in Mitotic Bookmarking. *PLoS Genet* **10**, e1004204 (2014).
48. Tempera, I. *et al.* Identification of MEF2B, EBF1, and IL6R as Direct Gene Targets of Epstein-Barr Virus (EBV) Nuclear Antigen 1 Critical for EBV-Infected B-Lymphocyte Survival. *J Virol* **90**, 345 (2016).